IOP Conf. Series: Journal of Physics: Conf. Series **822** (2017) 012006 doi:10.1088/1742-6596/822/1/012006

Influence of non perfect impedance boundary on the bistable region in thermoacoustic interactions

B Mohan[1] and S Mariappan[2]

Department of Aerospace Engineering, Indian Institute of Technology Kanpur, Kanpur-208016, India

[1] Graduate Student and Corresponding author

[2] Assistant Professor

E-mail: [1] mbala@iitk.ac.in, [2] sathesh@iitk.ac.in

Abstract. We investigate the influence of non perfect impedance boundary on the bistable zone in thermoacoustic interactions of a horizontal Rijke tube. A wave based approach is used to obtain the nonlinear dispersion relation with frequency dependent impedance boundary condition. The location and the time delay in the response of the heater are considered as bifurcation parameters to obtain the stability boundaries. In the presence of non perfect impedance boundary condition, we find that the extent of globally unstable regime reduces and the bistable zone significantly increases. The quantitative changes in the stability boundaries and the bistable zone are investigated for different time lags. However, the nature of bifurcation remains sub critical and unaltered for the range of time delays considered in the present study.

1. Introduction

Thermoacoustic instability is one of the major issue which has been faced by scientist, engineers and industrialist over the last five decades. Starting from rocket engines to gas turbines, boilers, afterburners and incinerators, thermoacoustic instability has influenced their operational limits. Controlling this instability during design phase is still a challenging task. Detailed review on the dynamics and control of this phenomenon can be found in [1, 2]. Rijke found that when heated gauze is placed at quarter length of a vertical tube in the bottom half, produced sound and this was later known as thermoacoustic instability [3].

Most of the study in thermoacoustic interactions concerned about different types of heat sources and their influence on the stability. The amplitude of the limit cycle oscillations is determined by the balance between the acoustic driving caused due to the unsteady heat release rate and damping in the system. Energy losses due to acoustic radiation and dissipation at the walls are the major sources of damping. Only few included radiation losses directly into analysis [4, 5, 6] and a few others added the effects of damping implicitly in energy equation [7, 8]. However, no detailed investigation on the effects of radiation losses on the stability regimes is performed yet. Thermoacoustic system possess three different stability regimes namely globally stable, globally unstable and bistable regions [5, 10, 11, 8]. In the globally stable zone, all the disturbances decay exponentially irrespective of the amplitude of oscillation and eventually, the system reaches its steady state. In the globally unstable zone, disturbances grow even if it is infinitesimally small; there is no linearly stable state and finite amplitude oscillation (limit cycle) prevails. In the bistable zone, the system dynamics relies completely on the initial perturbation

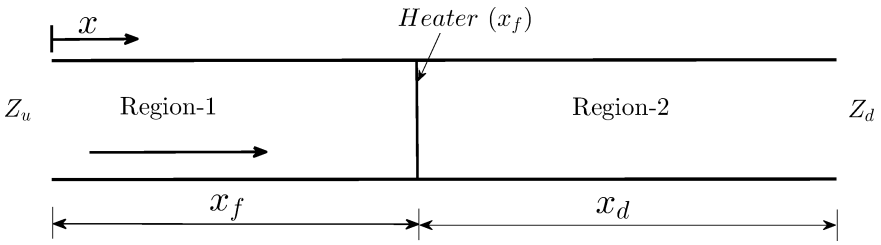

Figure 1. Schematic of Rijke tube.

given to the system [12]. This is manifested as an hysteresis in the experiments. Furthermore, classical linear stability analysis is not valid in this zone, making the prediction on the dynamics difficult. Since the bistable zone possesses crucial dynamics such as triggering and lies in between the linearly stable and linearly unstable zones, it is interesting to explore it in detail.

The presence of noise on the dynamics of the bistable zone was investigated exhaustively in the recent past. Experimental investigation in a simulated gas turbine combustor reported that inherent noise in the combustor can make nominally stable combustor into unstable [13]. Waugh et al. [15] found that high amplitude low frequency (pink) noise has strong influence on triggering. Experimental investigation of noise induced transition in a diffusion flame was performed by inducing random disturbances in fuel flow. A reduction in the amplitude of limit cycle oscillation was observed [16]. In reference [14], it was found that the system exhibits completely different type of bifurcation above certain threshold noise level. All the above investigations indicate that the nature of bifurcation or in turn the extent of the various stability regimes were altered significantly in the presence of noise.

We believe that the extent of bistable zone is not only affected by the noise, but also by the presence of acoustic losses in the system. Therefore our main objective in this study is to investigate the effects of radiation losses on the bistable zone, which are not given due attention in the past. Radiation losses in flanged and unflanged tubes, their dependence on frequency and amplitude were investigated in references [17, 18]. In this paper, describing function (DF) technique is used to predict the nonlinear stability of thermoacoustic oscillations. This technique is preferred, as it is easily possible to incorporate non perfect impedance boundary conditions. In the past, this framework was used to predict limit cycle, triggering and frequency of oscillations [10, 11, 4].

This paper is arranged in the following manner. Section 2 deals with the theoretical modeling of Rijke tube and obtaining the dispersion relation, followed by section 3 interpreting the results. In the end, section 4 provides a summary of the present work.

2. Modeling system dynamics using wave approach

One of the most simple and elegant model to capture the salient dynamics associated with thermoacoustic interactions is a Rijke tube and it is best suited for our study. Linearized acoustic momentum and energy equations govern the flow properties in a Rijke tube. Figure 1 shows the schematic of a Rijke tube with a heat source located at x_f. The heat source is assumed to be compact compared to the length of the tube l. The steady flow is from left to right and the associated Mach number is small. The mathematical model for heat source is obtained from Heckl [6]. As shown in figure 1, region 1 and 2 has constant flow properties. Linearized momentum and energy equations are combined to obtain the wave equation as described in reference[5],

$$\frac{\partial^2 p'}{\partial t^2} + \zeta \frac{\partial p'}{\partial t} - c^2 \frac{\partial^2 p'}{\partial x^2} = \frac{(\gamma - 1)}{S_c} \frac{\partial \dot{Q}'}{\partial t} \delta(x - x_f) \tag{1}$$

where p', $\dot{Q}'$, S_c, γ, ζ and δ denotes acoustic pressure in the duct, fluctuating heat release rate from the heat source, cross sectional area, ratio of specific heat capacities, acoustic damping and Dirac delta function respectively. The above equation (1) is solved using wave based approach [19]. The pressure and velocity fluctuations are represented as $p' = \Re\left[\hat{p}(x)exp(i\omega t)\right]$ and $u' = \Re\left[\hat{u}(x)exp(i\omega t)\right]$, $i = \sqrt{-1}$, where ω is the complex frequency with $\omega = \omega_r + i\omega_i$. ω_r and ω_i represent the oscillating circular frequency and the growth/decay rate of the oscillations respectively. These expressions are then inserted in the above equation to obtain an Helmholtz equation. Solving Helmholtz equation results in a solution for $\hat{p}$ and $\hat{u}$ as follows,

$$\hat{p}_n(x) = A_n \ exp\left[is_n\left(x - x_f\right)\right] + B_n \ exp\left[-is_n\left(x - x_f\right)\right] \quad (2)$$

$$\hat{u}_n(x) = -\frac{s_n}{\omega\rho_n}\{A_n \ exp\left[is_n\left(x - x_f\right)\right] - B_n \ exp\left(-is_n\left(x - x_f\right)\right)\} \quad (3)$$

For locations in the up ($0 \leq x < x_f$) and downstream ($x_f < x \leq l$) of the heat source, the subscripts n is replaced with u and d respectively. c_n is the local speed of sound and $s_n^2 = (\omega^2 - i\zeta\omega)/c_n^2$. Note that the above solutions are valid for all $x \neq x_f$. At x_f, the acoustic jump conditions, $p'_u(x_f^-) = p'_d(x_f^+)$ and $u'_d(x_f^+, t) - u'_u(x_f^-, t) = (\gamma - 1)\dot{Q}'(t)/(\gamma S_c P)$ are applied. The superscripts $'$, $\hat{}$, $^-$, $^+$ denote fluctuating quantities, complex amplitude, quantities just up and downstream of the heat source respectively. In the velocity jump condition, $\dot{Q}'(t)$ is replaced with describing function. This describing function assumes weak nonlinearity, meaning that only the response in the excitation frequency is used for the analysis and the higher harmonics are neglected. Furthermore, A_n, B_n are all constants and are eliminated to obtain the following nonlinear dispersion relation.

$$\xi\left[G_d\cos(s_d x_d) - iH_d\sin(s_d x_d)\right]\left[H_u\cos(s_u x_f) + iG_u sin(s_u x_f)\right] - \left[G_u\cos(s_u x_f)\right.$$
$$\left. + iH_u\sin(s_u x_f)\right]\left[H_d\cos(s_d x_d) - iG_d\sin(s_d x_d)\right]\left[1 + \frac{(\gamma-1)\dot{Q}}{\gamma S_c P u_u}\mathcal{F}\right] = 0 \quad (4)$$

Here $x_d = l - x_f$, $G_n = I_n - 1$, $H_n = I_n + 1$ and $I_n = \left(s_n/k_n - 1/Z_n\right)/\left(s_n/k_n + 1/Z_n\right)$. Further $\xi = \rho_u c_u/\rho_d c_d$ and $\mathcal{F}\left(u_u^-, \omega\right) = (\dot{Q}'/\dot{Q})/[u'_u(x_f^-)/u_u] = \mathcal{G} \ exp\left(i\phi\right)$. Z, P, $\mathcal{F}$, $\mathcal{G}$, ϕ represent acoustic impedance at the boundary associated with n (for instance when $n = u$, $Z_n = Z_u(\text{at } x = 0)$), steady state pressure, describing function, gain and phase. The expression for damping is taken from references [7, 18], $\zeta = \omega_r/\pi\left(c_1\omega_r/\omega_{r1} + c_2\sqrt{\omega_{r1}/\omega_r}\right)$. c_1 and c_2 are damping co-efficients which accounts for the losses. ω_{r1} denotes fundamental oscillation frequency of an organ pipe.

In equation (4), $\mathcal{F}$ represents the response of the heat source to various input frequencies and amplitude of velocity fluctuations. In this paper, the heat source is considered to be an electrical heater. The instantaneous heat transfer (release) rate ($\tilde{\dot{Q}}$) for a given unsteady velocity fluctuation is obtained from modified King's law [6].

$$\tilde{\dot{Q}} = L_w\left(T_w - T_u\right)\left\{X + 2\sqrt{\pi X c_v \rho u_u \frac{d}{2}}\left[\left(1 - \frac{1}{3\sqrt{3}}\right) + \frac{1}{\sqrt{3}}\sqrt{\left|\frac{1}{3} + \frac{u'_u\left(x_f^-, t - \tau_w\right)}{u_u}\right|}\right]\right\} \quad (5)$$

where L_w, T_w, T_u, d, X, c_v and ρ represent the wire length, wire surface temperature, upstream temperature, wire diameter, thermal conductivity, specific heat at constant volume and steady state density of the flow respectively. From equation (5), steady state heat transfer rate ($\dot{Q}$) is found by putting $u'_u = 0$ and the fluctuating heat transfer rate($\dot{Q}'$) is obtained from $\dot{Q}' = \tilde{\dot{Q}} - \dot{Q}$.

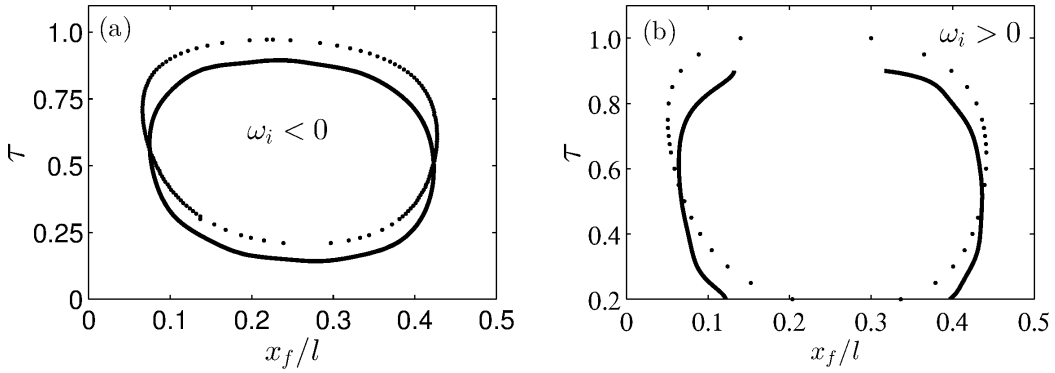

Figure 2. (a) Linear stability boundary and (b) nonlinear stability boundary in the $x_f/l - \tau$ plane. ω_i shown, is obtained in the limit $|u'_u(x_f^-)| = 0$. Further —— and ····· lines denotes the study of Subramanian et al. [8] and present analysis respectively. The non dimensional heat release rate $Q_{ND} = 0.8$.

Non dimensionalized fluctuating heat transfer rate is written as $Q_{ND} = (\gamma - 1)\dot{Q}/(\gamma S_c P u_u)$. τ_w is the time lag between the input u'_u and the response $\dot{Q}'$. It is non dimensionalized as $\tau = \tau_w c_u/l$.

Table 1. Parameters used in this investigation.

T_w=700 K	T_u=295 K	u_u=0.24 m/s	γ =1.4	R=288.35 J/kg K	l= 1 m
d=0.45 mm	L_w=13 m	r_t=52.5 mm	P=1atm	$c_1 = 0.1$	$c_2 = 0.06$

3. Results and discussion

In this section, results from the above solution procedure are first compared with the previous analysis [8], where the solution was obtained in the time domain using continuation methods. Acoustically perfect boundary conditions (open-open in this case) were used for the comparison. In perfect boundary conditions, the time averaged acoustic intensity is zero and hence there are no radiation losses. Later, the effects of inclusion of non perfect impedance boundary condition, which is the main objective of the present paper is discussed.

For a given x_f, acoustically open-open boundary condition ($Z_n = 0$) and other parameters shown in table 1, equation 4 is solved to obtain ω. From the complex frequency, both stability boundary and frequency of oscillations are obtained. To facilitate a one to one comparison with reference [8], ξ is kept 1 (although not true in reality) and other parameters are chosen as the same value given in the above reference. The comparison is shown in figure 2 for the linear and nonlinear stability boundaries, where the non dimensional time lag τ and heater location x_f/l are the parameters. The system is linearly stable, when $\omega_i > 0$ in the limit $|u'_u(x_f^-)| = 0$ and linearly unstable when $\omega_i < 0$. The demarcation line is the linear stability boundary. On the other hand, in the bistable zone, ω_i equals zero for two values of $|u'_u(x_f^-)| > 0$. At these two locations, when $d\omega_i/d(u'_u(x_f^-)) < 0$, there is an unstable limit cycle. Otherwise, a stable limit cycle occurs. As x_f is varied, these two solutions merge to form a *fold point* (in the parlance of dynamical systems' theory). The locus of this fold point in the $x_f/l - \tau$ plane forms the nonlinear stability boundary. The region between the linear and nonlinear stability boundaries forms the bistable zone.

We compare the boundaries obtained from this paper (dotted lines), with those from reference [8] (full lines) and are shown in figure 2. It is expected to have a perfect match between the two

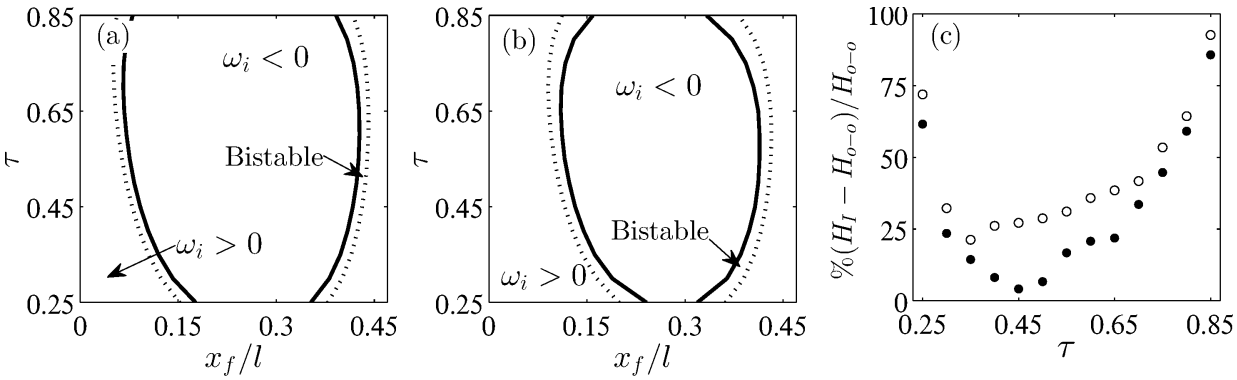

Figure 3. Stability boundaries for (a) perfect (acoustically open) (b) non perfect boundary conditions. —— and ····· lines indicate linear and nonlinear stability boundaries respectively. (c) Relative change in the extent of the bistable zone between figures 3 (a) and (b). ○ and ● denote left and right envelopes of stability boundaries respectively. $Q_{ND} = 0.95$.

results, as the equations, boundary conditions and the parameters are the same. We only observe that the stability boundaries are analogous qualitatively, they are different quantitatively. This difference is attributed to the different analysis methods used in both the investigations. In reference [8], Galerkin approach was used to convert the partial differential equation (1) to a set of ordinary differential equations and later continuation algorithm was used to obtain the stability boundaries. In the present investigation, we use wave based approach to predict the same. Both the methods use different approximations. In the former, since Galerkin spatial decomposition is used, the acoustic velocity jump across the heat source is excluded, while in the latter, higher harmonics in the describing function for the heat source are neglected.

Furthermore, for a given location of the heat source (say $x_f/l = 0.25$), the system is linearly and nonlinearly stable for low values of τ. As τ is increased, it crosses the stability boundaries, enters initially the bistable region and then linearly unstable zone. Further, as τ is increased to large values, the system again becomes globally stable. τ is related (approximately) inversely to the mass flow rate in the system. This phenomenon of a initially globally stable system becoming unstable and then becoming again stable, as the mass flow rate is increased is also observed in the experiments [9]. Hence, the present solution procedure is able to capture the observed trends in the experiments and compares qualitatively with the previous numerical investigations.

We can now use this model and the analysis procedure to investigate the effects of non perfect impedance boundary conditions. Frequency dependent impedance boundary conditions for an unflanged pipe is used from reference [17] for our investigation.

$$Z_n = \left.\frac{\hat{p}}{\hat{u}}\right|_n = \left(\frac{\omega_r r_t}{2c}\right)^2 - 0.6i\frac{\omega_r r_t}{c} \tag{6}$$

where, r_t is the radius of tube. This expression is included as Z_n in the dispersion relation (4) and solved for the complex frequency, thereby obtaining the stability boundaries. The obtained stability boundaries are then compared with those obtained by using perfect (open) boundary conditions (figure 3(a,b)). First, one could observe a reduction in the globally unstable zone (boundaries in full lines shown in both the figures). Non perfect impedance boundary conditions lead to additional losses due to acoustic radiation and hence the size of the unstable zone is decreased. For the same reason, the size of the globally stable zone, indicated by the nonlinear stability boundary (shown as dotted lines) is also increased. However, non trivially, region between the two boundaries (bistable zone) is increased.

One can observe two branches of the bistable zone in figure 3(a,b). These are indicated as left and right envelopes. The percentage relative change in the bistable zone due to the inclusion of the non perfect boundary conditions for both the envelopes are shown in figure 3(c). H_I and H_{o-o} denote the size of the bistable zone corresponding to non perfect impedance and acoustically open boundary conditions respectively. The increase in the size of bistable zone is significant and it varies with τ. The non monotonic trend with τ is because of the phase relation between heat release rate and pressure oscillation which in turn is related to the stability boundaries. The changes are more noticeable for the left envelope, where the values of x_f/l is close to the end, where a non perfect boundary condition is applied. However, the nature of bifurcation remained a sub critical Hopf in both the cases. The results indicate that the inclusion of non perfect impedance boundary condition leads to significant (on an average 25%) increase in the bistable zone. Hence, incorporation of correct impedance boundary conditions is essential to obtain accurate stability maps and thus the operating regimes of practical gas turbine combustors.

4. Conclusion

Stability analysis of thermoacoustic interactions in an electrically heated horizontal Rijke tube is performed. The dynamics of the heat source is modeled using modified King's law. Describing function analysis is then used to obtain the stability boundaries. A good qualitative comparison in the results with the previous investigations corresponding to the acoustically open-open boundary condition is observed. The analysis is extended to include non perfect impedance boundary conditions and the results are compared with those from acoustically open boundary conditions. From the obtained linear and nonlinear stability boundaries, we found that the inclusion of non perfect impedance boundary condition leads to an increase in the extent of globally stable regime and a decrease in the globally unstable regime. The major finding of this investigation is the *non trivial* increase in the extent of the bistable zone while incorporating non perfect impedance boundary conditions. However, there is no change in the observed nature of bifurcation. Relative change in the extent of the bistable zone is significant and exhibits a non monotonic variation with time lag. In conclusion, it is essential to include the correct non perfect impedance boundary condition to accurately predict the stability maps of thermoacoustic oscillations.

References

[1] Dowling A P and Morgans A S 2005 *Annu. Rev. Fluid Mech.* **37** 151-82
[2] Candel S 2002 *Proc. Combust. Inst.* **29** 1-28
[3] Rijke P L 1859 *Philo. Mag.* **17** 419-22
[4] Li J and Morgans A S 2015 *J. Sound Vib.* **346** 345-60
[5] Matveev K I 2003 *J. Fluid. Struct.* **18** 783-94
[6] Heckl M A 1990 *Acustica* **72** 63-71
[7] Matveev K I and Culick F E C 2003 *Combust. Sci. Tech.* **175** 1059-83
[8] Subramanian P, Mariappan S, Wahi P and Sujith R I 2010 *Int. J. Spray Combust.* **2** 325-56
[9] Mariappan S, Sujith R I and Schmid P J 2015 *Int. J. Spray Combust.* **7** 315-352
[10] Noiray N, Durox D, Schuller T and Candel S 2008 *J. Fluid Mech.* **615** 139-67
[11] Boudy F, Durox D, Schuller T and Candel S 2011 *Proc. Combust. Inst.* **33** 1121-28
[12] Strogatz S H 2000 *Nonlinear Dynamics and Chaos: with applications to Physics, Biology, Chemistry and Engineering* (Westview Press)
[13] Lieuwen T C 2002 *J. Prop. Power* **18** 61-7
[14] Gopalakrishnan E A and Sujith R I 2015 *J. Fluid Mech.* **776** 334-53
[15] Waugh I, Geuss M and Juniper M 2011 *Proc. Combust. Inst.* **33** 2945-52
[16] Jegadeesan V and Sujith R I 2013 *Proc. Combust. Inst.* **34** 3175-83
[17] Levine H and Schwinger J 1948 *Phys. Rev.* **73** 383-406
[18] Peters M C A M, Hirschberg A, Reijnen A J and Wijnands A P J 1993 *J. Fluid Mech.* **256** 499-534
[19] Dowling A P and Stow S R 2003 *J. Prop. Power* **19** 751-64